J|A|C|S
COMMUNICATIONS

Published on Web 05/02/2007

Ultrafast Energy Transfer within Cyclic Self-Assembled Chlorophyll Tetramers

Richard F. Kelley, Randall H. Goldsmith, and Michael R. Wasielewski*

Department of Chemistry and International Institute for Nanotechnology, Northwestern University, Evanston, Illinois 60208-3113

Received March 1, 2007; E-mail: m-wasielewski@northwestern.edu

Ever since the crystal structure of the LHII antenna protein from purple photosynthetic bacteria revealed that bacteriochlorophylls arrayed in a ring structure are used for light harvesting,[1] considerable effort has been invested in making biomimetic chromophore rings, which offer insights into the photophysics of energy collection and transfer in photosynthetic proteins.[2] Several synthetic structures comprising covalently linked metalloporphyrins display interchromophore energy transfer rates comparable to those observed in natural light harvesting proteins.[2] However, a more efficient strategy for multichromophore array construction is desirable for developing artificial photosynthetic systems for solar energy conversion. Studies of a self-assembled, porphyrin-based tetramer reveal that the rate of energy transfer between the porphyrins is 100 times slower than those of analogous covalent structures.[3] We have now prepared a zinc chlorophyll (ZC) derivative, **1**, that self-assembles into a cyclic tetramer and exhibits intramolecular energy transfer rates comparable to those observed for covalent ring structures. The larger transition dipole moment for the lowest energy electronic transition of the ZCs compared to that of the porphyrins increases the rate of Förster (through-space) energy transfer between the chlorophylls.

Compound **1** was synthesized in 50% yield using established Suzuki coupling methodology (see Supporting Information).[4] The ground-state absorption spectrum of **1** in pyridine reveals Soret (433 nm) and Q_y (660 nm) bands typical of ZC species, Figure S1. In toluene, the Soret band shifts to 434 nm, and the Q_y band shifts to 667 nm. These shifts are likely due to exciton coupling between two or more ZC molecules as a consequence of aggregate formation in the non-coordinating solvent.[5]

The aggregate structure was elucidated using small-angle X-ray scattering (SAXS) measurements performed on 10^{-5} M toluene solutions of **1** using a high-flux synchrotron source (Advanced Photon Source at Argonne National Laboratory). The solution-phase scattering pattern was obtained for the q region, 0.01 Å^{-1} < q < 1.9 Å^{-1}, Figure 2A. In the low-resolution scattering region (q < 0.2 Å^{-1}), the scattering intensity follows the Guinier relationship, $I(q) = I(0)\exp(-q^2R_g^2/3)$, which is parametrized in terms of the forward scattering amplitude, $I(0)$, and the radius of gyration, R_g.[6] The linearity of the Guinier plot between 0.01 Å^{-2} < q^2 < 0.02 Å^{-2} , Figure 2A insert, indicates that the sample consists of monodisperse structures,[7] thereby eliminating an extended stair-step structure which would likely be polydisperse in size. The least-squares fit to the linear data reveals a radius of gyration of 7.75 Å. The monodisperse nature of $\mathbf{1_4}$ in toluene allows direct comparisons between reciprocal-space scattering patterns and real-space molecular models through atomic pair distribution function (PDF) analysis. The experimental PDF for $\mathbf{1_4}$ in toluene was obtained using the X-ray scattering fitting program GNOM, Figure 2B.[8] The peaks in the PDF at 9.8 and 13.5 Å are the result of atom pair correlations between the nearest neighbor and next-nearest neighbor pairs, respectively.[9] MM+ geometry optimized models[10] of $\mathbf{1_4}$ reveal average Zn−Zn distances of 9.4 and 13.3 Å for the analogous pair correlations. The theoretical value of R_g obtained for each of these models was 7.3 Å.[11] The structure of the aggregate was also independently verified by replicating the raw scattering data using an ab initio simulated annealing procedure, Figure 2C.[12] The dimensions and shape determined using both PDF analysis and simulation strongly correlate with a cyclic, tetrameric aggregate.

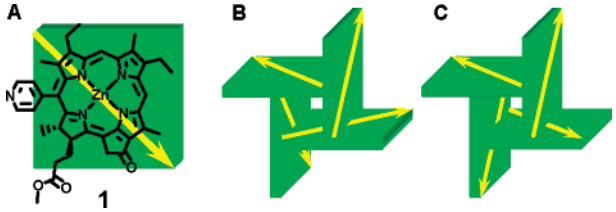

Figure 1. (A) Structure of **1**; (B) tetramer $\mathbf{1_4}$ with a transition dipole orientation which minimizes the steric repulsion of the propionic esters; (C) Tetramer $\mathbf{1_4}$ with a transition dipole orientation that minimizes the ground-state dipole moment of the aggregate.

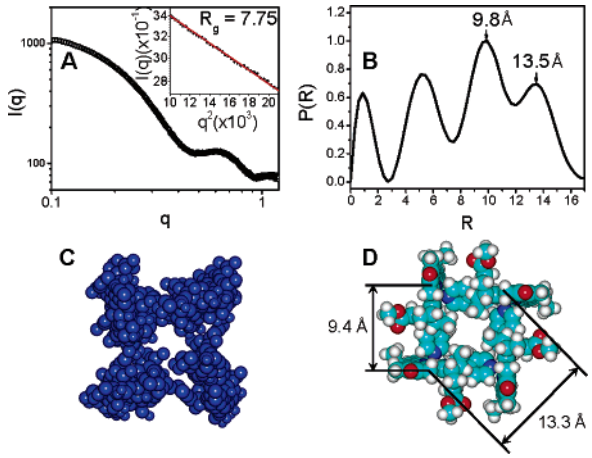

Figure 2. (A) Experimental scattering intensity, $I(q)$, versus scattering length vector, q, data for **1** in toluene (5×10^{-5} M) solution (0.1 Å^{-1} < q < 1.9 Å^{-1} region); (inset) scattering intensity versus q^2 for the same sample (0.01 Å^{-2} < q^2 < 0.02 Å^{-2} region). Guinier fit to the data is also shown; (B) atomic pair distribution functions (PDFs) for **1** in toluene obtained using the program GNOM; (C) the structure reconstructed from SAXS data; (D) MM+ geometry optimized structure of $\mathbf{1_4}$.

The resolution of the SAXS experiment ($d = 2\pi/q_{max}$) does not reveal the absolute configuration of the ZCs in $\mathbf{1_4}$ and unfortunately the ^{1}H NMR spectrum of $\mathbf{1_4}$ in toluene is severely broadened. Unlike the analogous porphyrin tetramer, $\mathbf{1_4}$ is composed of four enantiomerically pure, chiral ZC molecules. Steric arguments can be used to eliminate all but two structural possibilities. The structure shown in Figure 1B exhibits the least steric repulsion because all the propionic ester tails extend away from the assembly center, while the structure depicted in Figure 1C displays the smallest ground-state dipole moment as a result of cancellation of opposing ground-state dipoles.

10.1021/ja071362a CCC: $37.00

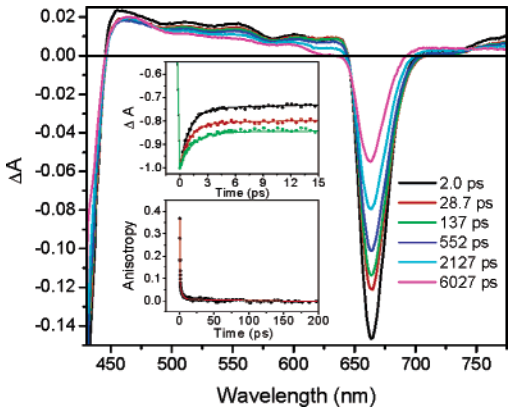

Figure 3. Transient absorption spectra of $\mathbf{1_4}$ in toluene following excitation with 665 nm, 120 fs laser pulses. The top inset shows the power-dependent transient absorption kinetics of $\mathbf{1_4}$ monitored at 660 nm using 1.00 (black line), 0.66 (red line), and 0.33 (green line) μJ per 665 nm excitation pulse. The bottom inset shows the transient anisotropy kinetics at 555 nm.

Förster energy transfer rates are highly dependent on the relative orientations of the transition dipole moments of the chromophores engaging in energy transfer.[13] The ZC transition dipole moment lies approximately along the N−N line shown in Figure 1, so that the orientations of the dipoles will vary depending on the orientations of the chromophores within the tetramer. Therefore, the relative orientations of the ZCs in $\mathbf{1_4}$ can be inferred using energy transfer considerations. The Förster model is approximate because the interchromophore distances in $\mathbf{1_4}$ are comparable to the extent of the transition dipoles. Nevertheless, the competing Dexter mechanism[14] involving direct orbital overlap or through-bond interactions between the ZCs in $\mathbf{1_4}$ should be less favorable because the HOMO orbital density of **1** at the Zn-center is negligible,[3,15] and the π-orbitals of adjacent monomers are nearly orthogonal.

Excitation of $\mathbf{1_4}$ in toluene with 665 nm, 120 fs laser pulses yields the transient absorption spectrum of its lowest excited singlet state $^{1*}\mathbf{1_4}$, Figure 3, which decays biexponentially with $\tau = 1.0 \pm 0.1$ ps and 3.8 ± 0.1 ns. Excitation of **1** in pyridine yields very similar transient absorption spectra for $^{1*}\mathbf{1}$, Figure S2, which decay monoexponentially with $\tau = 3.8 \pm 0.1$ ns. The 3.8-ns decay component in the transient absorption decay kinetics of both $^{1*}\mathbf{1}$ and $^{1*}\mathbf{1_4}$ matches the fluorescence lifetime of $^{1*}\mathbf{1}$ in pyridine, Figure S3. The amplitude of the 1.0-ps component in the decay of $^{1*}\mathbf{1_4}$ is laser-power dependent and indicative of singlet−singlet annihilation (Figure 3, inset). The time constant for energy transfer between adjacent chromophores in $\mathbf{1_4}$, τ_h, can be derived from the annihilation lifetime, τ_a, using the formula $\tau_a = \tau_h/(8 \sin^2(\pi/2N))$ developed for cyclic arrays of N chromophores with identical microscopic rate constants.[16] Using this model, $N = 4$, and the measured value of τ_a, $\tau_h = 1.2 \pm 0.1$ ps. Transient anisotropy measurements on $^{1*}\mathbf{1_4}$ confirmed this result ($\tau_h = 1.3 \pm 0.1$ ps) (Figure 3, inset and Figure S7, Supporting Information).

The orientation of the ZC transition moments in Figure 1B predict that the microscopic rate constants for Förster energy transfer between adjacent chromophores will be identical. In addition, the cross-diagonal energy transfer rates should be significantly slower than those between adjacent chromophores owing to the unfavorable orientation of the transition dipoles. Consequently, a monoexponential rate constant for annihilation is predicted. In contrast, the adjacent chromophores in Figure 1C exist in two conformations with respect to each other. Therefore two microscopic energy transfer rates contribute to the overall annihilation rate. To further investigate this case, kinetic models were created to include multiple nonequivalent microscopic rate constants (Figure S4). Numerical solutions to these kinetic schemes yield multiexponential kinetics for the annihilation process and simulations reveal that a ratio of $k_{EnT1}/k_{EnT2} > 5$ is sufficient to observe multiexponential annihilation kinetics. Our calculations of Förster energy transfer rates (Table S1) predict a ratio of $k_{EnT1}/k_{EnT2} > 15$. From this we conclude that the observed monoexponential annihilation kinetics preclude structure 1C.

The rate of energy transfer within $^{1*}\mathbf{1_4}$ is ~20 times faster than that observed for the self-assembled porphyrin tetramer, yet it is still ~10 times slower than the fastest rates observed in photosynthetic proteins. This is probably the result of the less than optimal alignment of the transition dipole moments in $\mathbf{1_4}$. We are currently exploring ways to self-assemble monodisperse chlorophyll antennas in which the transition dipole alignment leads to even faster energy transfer rates.

Acknowledgment. This paper is dedicated to Dr. Joseph J. Katz on the occasion of his 95th birthday. This work was supported by the Division of Chemical Sciences, Office of Basic Energy Science DOE under Grant No. DE-FG02-99ER14999. SAXS studies at the Advanced Photon Source were supported by Office of Science, Office of Basic Energy Sciences, DOE under Contract No. W-31-109-ENG-38. R.H.G. also thanks the Link Foundation and the Dan David Foundation for partial support.

Supporting Information Available: Experimental details, including synthesis and characterization of **1**, UV−vis and transient absorption/anisotropy spectra, and rate expressions. This material is available free of charge via the Internet at http://pubs.acs.org.

References

(1) McDermott, G.; Prince, S. M.; Freer, A. A.; Hawthornthwaite-Lawless, A. M.; Papiz, M. Z.; Cogdell, R. J.; Isaacs, N. W. *Nature* **1995**, *374*, 517.
(2) (a) Rucareanu, S.; Schuwey, A.; Gossauer, A., *J. Am. Chem. Soc.* **2006**, *128*, 3396. (b) Shoji, O.; Tanaka, H.; Kawai, T.; Kobuke, Y., *J. Am. Chem. Soc.* **2005**, *127*, 8598. (c) Nakamura, Y.; Hwang, I.-W.; Aratani, N.; Ahn, T. K.; Ko, D. M.; Takagi, A.; Kawai, T.; Matsumoto, T.; Kim, D.; Osuka, A. *J. Am. Chem. Soc.* **2005**, *127*, 236. (d) Li, J.; Ambroise, A.; Yang, S. I.; Diers, J. R.; Seth, J.; Wack, C. R.; Bocian, D. F.; Holten, D.; Lindsey, J. S. *J. Am. Chem. Soc.* **1999**, *121*, 8927.
(3) (a) Yatskou, M. M.; Koehorst, R. B. M.; Donker, H.; Schaafsma, T. J. *J. Phys. Chem. A* **2001**, *105*, 11425. (b) Yatskou, M. M.; Koehorst, R. B. M.; van Hoek, A.; Donker, H.; Schaafsma, T. J.; Gobets, B.; van Stokkum, I.; van Grondelle, R. *J. Phys. Chem. A* **2001**, *105*, 11432.
(4) Kelley, R. F.; Tauber, M. J.; Wasielewski, M. R., *Angew. Chem., Int. Ed.* **2006**, *45*, 7979.
(5) Kasha, M.; Rawles, H. R.; El-Bayoumi, M. L. *Pure Appl. Chem.* **1965**, *11*, 371.
(6) (a) Glatter, O. *Neutron, X-ray, and Light Scattering*; Elsevier: Amsterdam, 1991. (b) Guinier, A.; Fournet, G. *Small Angle Scattering*; Wiley: New York, 1955.
(7) Svergun, D. I.; Koch, M. H. *Rep. Prog. Phys.* **2003**, *66*, 1735.
(8) Svergun, D. I. *J. Appl. Cryst.* **1992**, *25*, 495.
(9) (a) Tiede, D. M.; Zhang, R.; Chen, L. X.; Yu, L.; Lindsey, J. S., *J. Am. Chem. Soc.* **2004**, 126, 14054. (b) Lee, S. J.; Mulfort, K. L.; O'Donnell, J. L.; Zuo, X.; Goshe, A. J.; Wesson, P. J.; Nguyen, S. T.; Hupp, J. T.; Tiede, D. M. *Chem. Commun.* **2006**, 4581.
(10) *Hyperchem*, version 5.02; Hypercube Inc.: Gainesville, FL, 1997.
(11) Zhang, R.; Thiyagarajan, P.; Tiede, D. M. *J. Appl. Crystallogr.* **2000**, *33*, 565.
(12) Svergun, D. I. *Biophys. J.* **1999**, *76*, 2879.
(13) Lakowicz, J. R. *Principles of Fluorescence Spectroscopy*. 2nd ed.; Kluwer Academic: Dordrecht, The Netherlands, 1999; p 698.
(14) Dexter, D. L. *J. Chem. Phys.* **1953**, *21*, 836.
(15) Kelley, R. F.; Tauber, M. J.; Wasielewski, M. R. *J. Am. Chem. Soc.* **2006**, *128*, 4779.
(16) Trinkunas, G. *J. Lumin.* **2003**, *532*, 102−103.

JA071362A